DO NOT [illegible] COPY

[redacted]

DOWNGRADED [redacted] AR INTERVALS:
DECLASSI [redacted] TER 12 YEARS
D [redacted] R 5200.10

SINGLE COPY ONLY

Z65·11104

CLASSIFICATION CHANGE
To UNCLASSIFIED
By authority of [illegible]
Changed by [illegible] Date 12/31/72
Classified Document Master Control Station, NASA
Scientific and Technical Information Facility

MASSACHUSETTS INSTITUTE OF TECHNOLOGY

APOLLO

GUIDANCE AND NAVIGATION

Approved *Milton B. Trageser* Date 11/24/64
MILTON B. TRAGESER, ASSOCIATE DIRECTOR
APOLLO GUIDANCE AND NAVIGATION PROGRAM

Approved *Roger B. Woodbury* Date 12/2/64
ROGER B. WOODBURY, DEPUTY DIRECTOR
INSTRUMENTATION LABORATORY

(Unclassified Title)

R-466

VIBRATION EFFECTS ON APOLLO GUIDANCE

F. D. Grant

October 1964

[redacted]

INSTRUMENTATION LABORATORY

CAMBRIDGE 39, MASSACHUSETTS

COPY # 17 OF 195 COPIES
THIS DOCUMENT CONTAINS 36 PAGES

DO [illegible] COPY

[redacted]

ACKNOWLEDGMENT

This report was prepared under DSR Project 55-191, sponsored by the Manned Spacecraft Center of the National Aeronautics and Space Administration through contract NAS9-153.

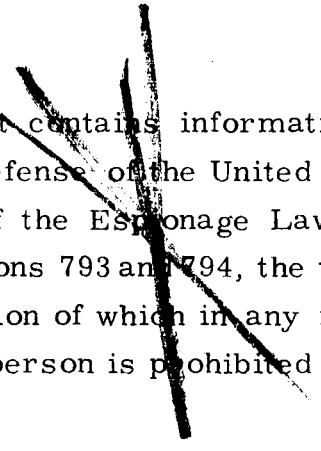

This document contains information affecting the national defense of the United States within the meaning of the Espionage Laws, Title 18, U. S. C., Sections 793 and 794, the transmission or the revelation of which in any manner to an unauthorized person is prohibited by law.

R-466

(Unclassified title)

VIBRATION EFFECTS ON APOLLO GUIDANCE

(Unclassified)

ABSTRACT

This report describes the significant effects of vibration on inertial component guidance performance. The transmission of linear and angular vibrations from spacecraft frame through the navigation base to the stable member is considered. Most significant vibration effects produce rectified errors that result in equivalent bias drift or bias error in a constant vibration field. Vibration effects on trajectory cutoff errors are presented for the different Apollo trajectories. The Appendix contains brief descriptions of the significant vibration effects on inertial components.

by Frederic D. Grant

October, 1964

TABLE OF CONTENTS

LIST OF TABLES

LIST OF FIGURES

VIBRATION EFFECTS ON APOLLO GUIDANCE

Introduction

This paper is concerned with determining and presenting the significant effects of spacecraft vibration on inertial component guidance performance for the various Apollo trajectories. We will not be concerned here with the effects of transient acceleration or of shocks, but rather with the problem of the effects of steady vibration of the spacecraft in the vicinity of the Navigation Base.

Figure 1 is a flow diagram showing the various error-producing effects of vibrations on the IMU gimbals and on the Stable Member gyros and accelerometers. This figure shows that the linear vibrations sensed by the inertial components are functions of the transmissibilities of the Navigation Base mounting and of the IMU gimbals. The angular vibrations sensed by the inertial components are functions of the torque response and of the base motion isolation response of the IMU gimbals servos as well as of the angular transmissibility of the Navigation Base.

Table 1 lists the principal vibration effects on IMU gimbals and on inertial components. The effects of angular vibration caused by base angular motion perturbations and by disturbing torques to the IMU gimbal servos will be described later.

Three of the linear vibration effects are caused by anisoelastic torques, all of which are a function of the acceleration squared. The fourth vibration effect is also a function of the acceleration squared, but where the two accelerations are 90° out of phase with each other producing a cylindrical motion. The angular vibration effects are actually the effects of Stable Member angular motion on the gyros. Except for gyro anisoinertia the resulting drift errors are due to kinematic effects in the presence of both in-phase and out-of-phase (coning) angular motions. Accelerometer sculling, which is caused by combined linear and angular in-phase vibration, is a rectified accelerometer cross-coupling error. All of the above effects give rise to rectified accelerometer or gyro drift errors and hence to average accelerometer indication

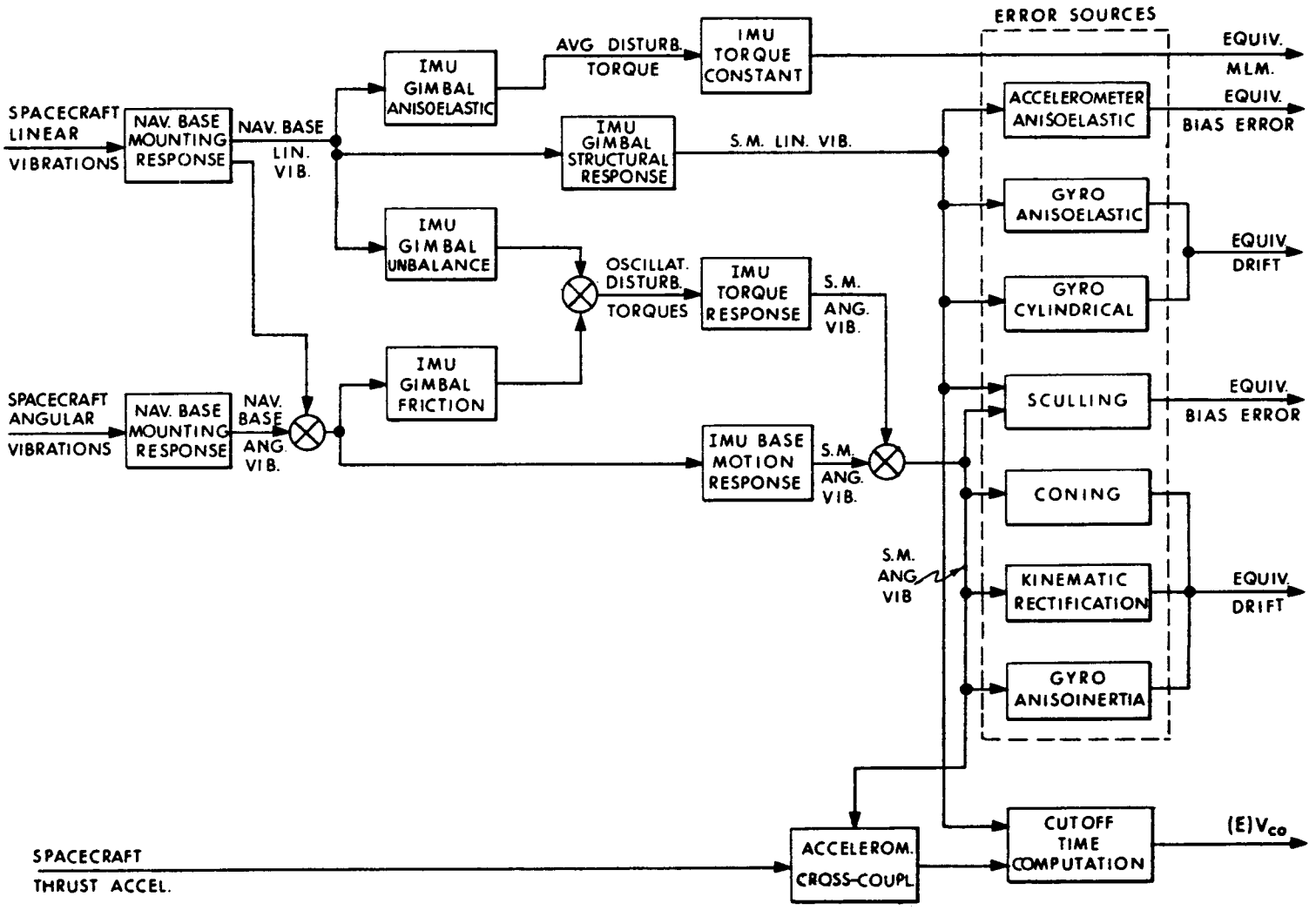

Fig. 1 Vibration effects on guidance errors.

TABLE 1

Vibration Effects on Inertial Components

A. Linear Vibration Effects
   a. IMU gimbal anisoelastic
   b. Gyro anisoelastic
   c. Gyro cylindrical motion
   d. Accelerometer anisoelastic

B. Angular Vibration Effects
   a. Gyro coning
   b. Gyro anisoinertia and kinematic rectification

C. Combined Linear-Angular Vibration Effects
   a. Accelerometer sculling

D. Cutoff Time Computation Effects
   a. Uncoupled vibration effects
   b. SM angular vibration effect

errors or to average gyro drift rates. The two effects in the last section are not rectification effects and are listed for their effect on cutoff time computation. All of these vibration effects are individually and briefly described in Appendix A.

Linear Vibration Transmission

Before specifically analyzing the effects of vibrations on the Stable Member inertial components, the transmission of linear and angular vibrations from the spacecraft to the Stable Member via the Navigation Base and the IMU gimbals must first be considered.

Earlier mounting designs for the Navigation Base for both the CM and the LEM contemplated the use of relatively soft-mounted vibration isolation systems whose maximum transmissibility would be about 4 at 30 cps and which would effectively attenuate all accelerations above 50 cps. However, present design for the LEM (and perhaps for the CM) is a nonelastic strain isolation system. This would maintain alignment of the Navigation Base relative to spacecraft frame. However, the transmissibility to linear vibrations would be essentially unity.

The transmission of vibrations from the navigation base through the IMU gimbals and bearings to the Stable Member (or inner gimbal) should next be considered. The resonant frequencies of the gimbal assembly are complex functions of the gimbal stiffnesses and weights. Experimental tests show that the first resonant frequency occurs somewhere in the 125-to-150-cps region depending on the vibration axis. The transmissibility of this frequency had been determined to be about 20 for some early Block 1 systems, but lately this has been reduced to about 10. The transmissibilities for the higher resonant frequencies at 450, 650, and 1200 cps are all about 3 or 4. Much of the navigation base vibration energy will be transmitted to the Stable Member in the 125-to-150-cps region.

Angular Vibration Transmission

At present there are little data available on spacecraft angular vibrations near the navigation base. With soft-mounted vibration isolation mounting for the Navigation Base on the Command Module, the rms navigation base angular vibration has been estimated to be about 3 mr. This can be caused by either spacecraft angular or linear vibrations.

The effect of navigation base angular vibrations on inertial alignment of the Stable Member is a function of gimbal servo performance. Ideally, the three SM inertial gyros (IRIGs) together with the base motion isolation gimbal servos will keep the Stable Member orientation fixed with respect to inertial space in the presence of navigation base angular disturbances. Actually such disturbances as well as torque and other disturbances may cause angular vibrations of the Stable Member. The following table lists the principal potential causes of SM angular vibration.

TABLE 2

Causes of SM Angular Vibration

1.	Oscillatory torque due to linear vibration acting on IMU gimbal unbalance
2.	Oscillatory torque due to gimbal friction torques in the presence of oscillatory base motion rates
3.	SM oscillations due to base motion angular vibration and to servo motor back emf.

The present design for the IMU gimbal servos incorporates the use of high source impedance motor drives. When, for example, the IMU case rotates with respect to the outer gimbal generating a back emf in the servo motor, the existence of the high source impedance makes the gyro error signal effectively independent of the back emf and hence of case rotation disturbances. Hence, there should be no significant SM perturbations even for high vibration frequencies if the three gimbal axes are approximately orthogonal. For the trajectories studied here (except earth reentry) the gimbal axes will be orthogonal. Whenever large middle gimbal angles develop, causing the gimbal axes to be non-orthogonal, significant SM perturbations can result if vibration frequencies exceed the gimbal servo bandwidths.

These considerations show that torque disturbances are the only significant causes of SM angular oscillations for the guided trajectories studied here. Such disturbances can be caused by either IMU gimbal unbalance in the presence of linear vibrations or by gimbal friction torques. Figure 2 shows the torque response (angle out for torque in) of the 3 IMU gimbal servos as a function of frequency.

The IMU gimbal unbalance is estimated to be about 0.06 in. oz. about each gimbal axis in a 1-g field. However, even in a 10-g vibration field the resulting sinusoidal torque of 0.6 in. oz. is insignificant relative to the friction torques.

The sign of the friction torque is determined by the relative angular rate between, for example, gimbal and case for the outer gimbal axis. The following table lists estimates for the friction torques about the three gimbal axes. These are representative figures for most powered trajectories. From Figure 2 it can be seen that the peak SM oscillation for a given disturbing torque amplitude is reached in the vicinity of 16 cps (100 rad/sec). Table 3 lists the peak SM vibration amplitudes (zero to peak) corresponding to the estimated friction torques.

Later these SM angular vibrations will be used to compute the gyro coning and other errors. Note that these SM angular oscillations are independent of navigation base linear or angular vibration amplitudes and are only a function of frequency and friction torque. Because of the presence of vibrations it is expected that starting friction (stiction) will be approximately equal to running friction.

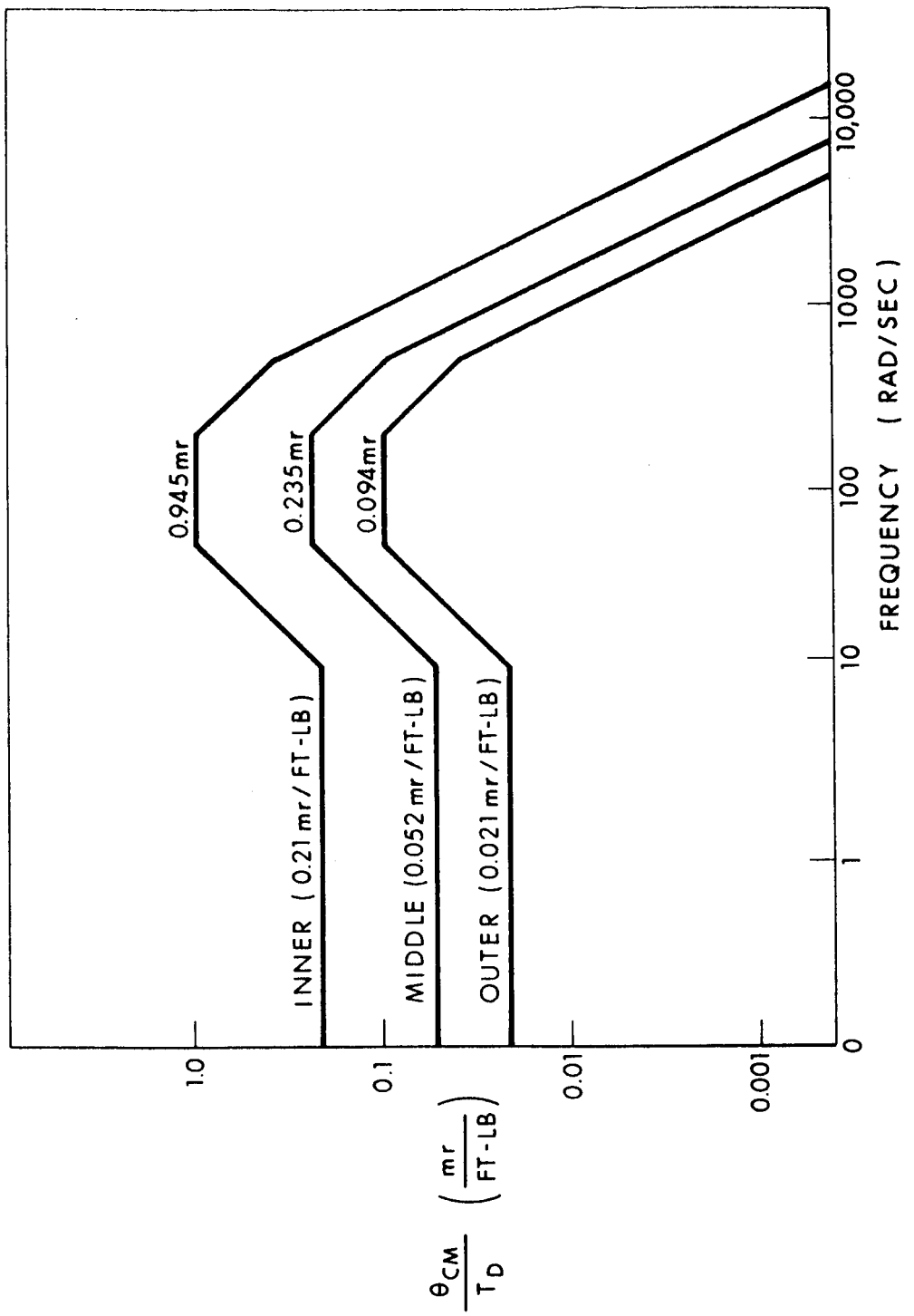

Fig. 2 IMU gimbal servo torque response curves vs frequency.

TABLE 3

SM Friction Torque Response

Gimbal Axis	Estim. Friction Torque	Peak SM Response
Outer	17 in. oz.	0.009 mr
Middle	10 in. oz.	0.012 mr
Inner	10 in. oz.	0.050 mr

Vibration Data

Having analyzed the transmission of vibration to the Stable Member, we are now ready to study and compute the effects of vibration on the SM inertial components themselves. Before embarking on this task, the vibration data problem should be discussed.

The ideal situation would be to have vibration data (preferably power spectral density vs. frequency) available for each of the Apollo CM trajectories and for the LEM trajectories. These data would be descriptive of conditions in the vicinity of the navigation base as a function of time for each powered trajectory. Such complete data will probably never be available, nor would they be necessary if the vibrations were of sufficiently low amplitude for all conditions.

At present only a limited amount of vibration data is available for the CM-SM and for the LEM configurations. None is available for earth reentry, or for the S-IV-B (translunar injection), and little is available for the earth launch to orbit trajectory.

In a constant vibration field most vibration effects on guidance errors are reducible to equivalent gyro bias drifts or to accelerometer bias errors. (See Appendix.) In order to use the error coefficients relating cutoff errors to bias errors and so reduce computational labor, it was assumed that vibration characteristics remained approximately constant for the powered trajectory duration for all trajectories studies. For the LEM and CM-SM trajectories, this is perhaps a reasonable assumption, since they occur outside the sensible atmosphere. However, for the earth launch to orbit trajectory, where vibrations are strong functions of such factors as dynamic pressure and velocity, the assumption of constant rms acceleration is indeed a drastic

simplification. However, since the greater part of the trajectory is above the sensible atmosphere such an assumption can be used as a first approximation, particularly where little vibration data are available. Later, when more complete and accurate vibration data for the different trajectories become available, the error tables will be recomputed and this report will be revised.

The following approximate estimates of rms linear vibration acceleration of the Stable Member for the different spacecraft configurations were used in computing the error tables. Approximate as these assumptions may be, they serve the useful purposes of:

1. indicating what the effects of guidance errors are for a particular rms acceleration level, and
2. indicating the relative significance of particular guidance error effects.

Since the more significant errors vary as the square of the vibratory acceleration, the effect of changing the rms acceleration level may be readily estimated.

TABLE 4

SM Vibration Acceleration Estimates

Spacecraft Configuration	Typical Trajectory	Estim. Rms Accel, g's	Vibration Energy Concentrated at
Sat. V	Earth Orbit Insert.	2.0	125 cps
S-IV-B	Translunar Injection	3.0	125 cps
CM-SM	Lunar Orbit Insert. Trans-earth Injection	3.1	125 cps
LEM	Descent, Ascent	7.6	125 cps
CM	Reentry	--	----

These acceleration estimates were based on the following available data. For the CM asymptotic curves for power spectral density near the navigation base vs. frequency for atmospheric and for space flight conditions were obtained from NAA/S&ID. Similar curves from GAEC gave estimates for the LEM near the navigation base. Computations for Table 4 assumed hard strain-free mounting of the navigation base to the spacecraft. Since the primary resonance of the IMU gimbals was at about 125 cps (where the maximum transmissibility was assumed to be 10), the power spectral density near 125 cps was of primary interest. (If the navigation base were soft-mounted, the mounting natural frequency of 30 cps would become the frequency of interest. Substitution of soft-mounting for hard-mounting would reduce rms acceleration transmitted to the SM by a factor of about 3.3 if the power spectral density were the same at both frequencies.) The rms acceleration estimates in Table 4 were based on the power spectral density estimates for the 125 cps region. The relatively high estimate of 7.6 g's for the LEM was based on a GAEC estimate of 0.059 g^2/cps for the PSD for this region. It was recognized that the GAEC curve represented an "envelope" curve that was based on data obtained from accelerometer measurements in a particular missile zone for an array of missiles. For this reason the above estimate was divided by two to yield hopefully a more representative estimate of power spectral density to arrive at the 7.6 g figure.

For earth orbit insertion trajectory the assumed rms acceleration of 2 0-g's was computed for space flight conditions (no sensible atmosphere) which prevail for Saturn V from 150 secs after launch to cutoff at 730 secs. The vibratory acceleration for the first 150 seconds is a strong function of the dynamic pressure which reaches a peak at about 80 specs, at which time it is about 10.8-g's rms. The time-varying acceleration implies time-varying guidance errors due to vibration. The present computation programs do not provide for such errors. Hence, as a rough approximation, an average 2.0-g's rms acceleration was assumed to exist for the first 150 seconds as well as for the rest of the flight.

For earth reentry trajectories the power spectral density of the vibration at peak acceleration is estimated to be about one-fourth that for atmospheric flight conditions during earth launch trajectory. The rms Stable Member acceleration is then about 3.4-g's. As for the first phase of earth launch the vibratory acceleration is a strong function of dynamic pressure

and velocity throughout reentry. Because of the lack of data for reentry vibration conditions and because the assumption of constant vibratory acceleration is a poor one for earth reentry, no attempt has been made at present to determine vibration error effects for reentry.

Vibration Effects Error Tables

Table 1 listed the significant error producing effects of vibrations of inertial components. Appendix A describes each error effect briefly. Therein it is shown that most error effects could be characterized as being equivalent to gyro bias drifts or to acceleromater bias errors for constant vibration input.

Table 5 is a typical computation table (for the CM-SM configuration trajectories - lunar orbit insertion and transearth injection). This table indicates for each vibration effect the computation steps for computing the equivalent gyro bias drifts or accelerometer bias errors or other errors. The computation tables for the other spacecraft configurations are identical to Table 5 except for the estimated rms acceleration level and hence are not presented here.

Table 6 through 11 give the position and velocity errors due to vibration effects on guidance for the following trajectories:

Table 6 - Earth Orbit Insertion (Saturn 5)
Table 7 - Translunar Injection (S-IV-B)
Table 8 - Lunar Orbit Insertion (CM-SM)
Table 9 - Transearth Injection (CM-SM)
Table 10 - Lunar Descent (LEM)
Table 11 - Lunar Ascent (LEM)

These tables use the values for the average equivalent guidance errors that had been computed in Table 5 and similar tables.

Comments on Error Tables

Inspection of these error tables shows that by far the most significant error producing effects of vibrations are:

(1) gyro anisoelasticity,
(2) accelerometer anisoelasticity, and
(3) accelerometer sculling.

For gyro anisoelasticity (or acceleration-squared sensitive gyro drift rate) the assumed drift sensitivity was 1 meru/g^2 for the error tables. This is actually a specification value, which should not be exceeded. If this is considered as equivalent to a 3-sigma uncertainty, the position and velocity errors due to gyro anisoelasticity in the various tables should be divided by three to give an rms error estimate. Gyro anisoelasticity is primarily a function of gyro design and assembly and should not vary much from unit to unit nor with time.

For accelerometer anisoelasticity the assumed g^2 sensitive indication error was 10 $\mu g/g^2$ (or, equivalently, 10 ppm/g or 0.01 cm/sec^2/g^2) for the error tables. This is also estimated to be roughly a 3-sigma uncertainty. This is a difficult error term to measure for the PIPA, even for steady acceleration inputs, and little data are presently available. Detailed tests have been under way for the last few months, but these have not yet been completed. The position and velocity errors in the various error tables should be divided by 3 to yield rms error estimates.

The other vibration effects are relatively small. Errors due to IMU gimbal anisoelasticity (see Table 5) were insignificant and were not listed in the other error tables. For the same reason a number of other error effects were not listed. Computation for uncoupled vibration effects on cutoff time were based on a rough estimate of 1-g (zero- peak) at cutoff in the 16 cps region where this has maximum effect.

A study of the error Tables 6 through 9, giving vibration effects on the CM's IMU for different trajectories, shows that the resulting rss error is relatively insignificant compared to the rss error due to guidance and initial condition errors; and the vibration error would be more insignificant if one-sigma gyro and accelerometer anisoelasticity error terms had been assumed.

However, Tables 10 and 11 show that vibrations have considerably more effect on the LEM's IMU. Here, because of the relatively high rms acceleration estimate (see Table 4 and its explanatory paragraphs) the equivalent bias drift is 58 meru and the equivalent accelerometer bias error is 0.57 cm/sec^2 when the 3-sigma estimates for component anisoelasticity are used. Truer rms estimates would be one-third these values or 19 meru and 0.19 cm/sec^2. Since these are by far the dominant error effects, the rss vibration error (for example, for the Decent Trajectory) becomes roughly a third of the rss error due to guidance and initial condition errors.

A) Linear Vibration Effects

Error Effect	Component	Error Term	RMS Error Value	Estim. RMS Vib. Accel. at comp.	Avge. Torque ft-lbs	Avge. Mlm. about gimbal axis	Avge. Equiv. Bias Error
IMU	OGA	Compliance Difference	$12\,\mu\frac{\text{inch}}{\text{lb}}$	3.1 g	0.010	$0.20(10^{-3})$mr	---
Gimbal	MGA	Compliance Difference	$11\,\mu\frac{\text{inch}}{\text{lb}}$	3.1 g	0.005	$0.26(10^{-3})$mr	---
Anisoelastic	IGA	Compliance Difference	$12\,\mu\frac{\text{inch}}{\text{lb}}$	3.1 g	0.003	$0.63(10^{-3})$mr	---
Gyro Anisoelastic	X Gyro	$A^2D_{(IA)(SA)X}$	$1\,\frac{\text{meru}}{g^2}$	3.1 g	---	---	9.6 meru
	Y Gyro	$A^2D_{(IA)(SA)Y}$	$1\,\frac{\text{meru}}{g^2}$	3.1 g	---	---	9.6 meru
	Z Gyro	$A^2D_{(IA)(SA)Z}$	$1\,\frac{\text{meru}}{g^2}$	3.1 g	---	---	9.6 meru
Gyro Cylindrical	X Gyro	Wheel-Float Compliance	$10\,\mu\frac{\text{inch}}{\text{lb}}$	3.1 g	---	---	0.05 meru
	Y Gyro	Wheel-Float Compliance	$10\,\mu\frac{\text{inch}}{\text{lb}}$	3.1 g	---	---	0.05 meru
	Z Gyro	Wheel-Float Compliance	$10\,\mu\frac{\text{inch}}{\text{lb}}$	3.1 g	---	---	0.05 meru
Accelero- meter Anisoelastic	X PIPA	NCXX	$10\,\frac{\mu g}{g^2}$	3.1 g	---	---	$0.096\,\frac{\text{cm}}{\text{sec}^2}$
	Y PIPA	NCYY	$10\,\frac{\mu g}{g^2}$	3.1 g	---	---	$0.096\,\frac{\text{cm}}{\text{sec}^2}$
	Z PIPA	NCZZ	$10\,\frac{\mu g}{g^2}$	3.1 g	---	---	$0.096\,\frac{\text{cm}}{\text{sec}^2}$

B) Angular Vibration Effects

Error Effect	Component	Estim. Vib. Amplitudes mr.	Vib. Freq. cps	Avge. Equiv. Bias Drift meru
Gyro Coning & In-Phase Motions	X Gyro	0.05-0.01	16	0.10
	Y Gyro	0.05-0.01	16	0.05
	Z Gyro	0.05-0.01	16	0.10

C) Linear-Angular Vibration Effects

Error Effect	Component	Estim. RMS Vib. Accel. at given Freq.	Est. RMS Ang. Vib.	Vib. Freq.	Avge. Equiv. Bias Error
Accelero- meter Sculling	X PIPA	0.3 g	0.05 mr	16 cps	$0.015\,\frac{\text{cm}}{\text{sec}^2}$
	Y PIPA	0.3 g	0.01 mr	16 cps	$0.003\,\frac{\text{cm}}{\text{sec}^2}$
	Z PIPA	0.3 g	0.05 mr	16 cps	$0.015\,\frac{\text{cm}}{\text{sec}^2}$

Table 5

Computation Table For CM-SM Trajectories
(Lunar Orbit Insertion and Transearth Injection)

Effect Class	Error Effect	Equiv. Guid. Error Term	Avge. Equiv. Guid. Error	Position Error in Target Axes in ft.			Velocity Error in Target Axes in ft/sec		
				Alt.	Track	Range	Alt.	Track	Range
Linear Vibration Effects	Gyro	BDX	4.0 meru		646			2.32	
	Anisoelastic	BDY	4.0 meru	558		478	2.42		1.00
	(1 meru/g^2)	BDZ	4.0 meru		94			0.22	
	Gyro	BDX	0.03 meru		5			0.02	
	Cylindrical	BDY	0.03 meru	4		4	0.02		0.01
		BDZ	0.03 meru		1			0	
	Accelero-	ACBX	0.04 $\frac{cm}{sec^2}$	340		156	1.07		0.43
	meter Aniso-	ACBY	0.04 $\frac{cm}{sec^2}$		314			0.83	
	elastic (10$\mu g/g^2$)	ACBZ	0.04 $\frac{cm}{sec^2}$	151		279	0.46		0.73
Angular Vibration Effects	Gyro	BDX	0.10 meru		16			0.06	
	Coning & In-	BDY	0.05 meru	7		6	0.03		0.01
	Phase Motion	BDZ	0.10 meru		5			0.01	
Linear-Angular Vibration Effects	Accelero-	ACBX	0.010 $\frac{cm}{sec^2}$	85		39	0.27		0.11
	meter	ACBY	0.002 $\frac{cm}{sec^2}$		16			0.04	
	Sculling	ACBZ	0.010 $\frac{cm}{sec^2}$	38		70	0.12		0.19
Cut-off Time Computation Effects	Uncoupled	$(E)V_{(alt)co}$	---ft/sec						
	Vibration	$(E)V_{(tk)co}$	---ft/sec						
	Effects	$(E)V_{(rge)co}$	0.07ft/sec						0.07
RSS Error due to Vibration Effects				676	740	581	2.70	2.47	1.33
RSS Error due to Guidance & Initial Condition Errors exculsive of Vibration Effects				3,895	11,770	2,410	14.47	30.52	6.43

Table 6

Earth Orbit Insertion Trajectory Cutoff Errors
Due To Vibration Effects On Guidance Errors

Effect Class	Error Effect	Equiv. Guid. Error Term	Avgc. Equiv. Guid. Error	Position Error in Target Axes in ft.			Velocity Error in Target Axes in ft/sec		
				Alt.	Track	Range	Alt.	Track	Range
Linear Vibration Effects	Gyro	BDX	9.0 meru		105			1.14	
	Anisoelastic	BDY	9.0 meru	105		24	1.20		0.24
	(1 meru/g^2)	BDZ	9.0 meru		21			0.30	
	Gyro	BDX	0.05 meru		1			0.01	
	Cylindrical	BDY	0.05 meru	1		0	0.01		0
		BDZ	0.05 meru		0			0	
	Accelero-	ACBX	0.09 $\frac{cm}{sec^2}$	132		60	0.87		0.39
	meter Aniso-	ACBY	0.09 $\frac{cm}{sec^2}$		141			0.90	
	elastic (10μg/g^2)	ACBZ	0.09 $\frac{cm}{sec^2}$	60		129	0.39		0.81
Angular Vibration Effects	Gyro	BDX	0.10 meru		1			0.01	
	Coning & In-	BDY	0.05 meru	0		0	0		0
	Phase Motion	BDZ	0.10 meru		0			0	
Linear-Angular Vibration Effects	Accelero-	ACBX	0.015 $\frac{cm}{sec^2}$	23		10	0.15		0.08
	meter	ACBY	0.003 $\frac{cm}{sec^2}$		4			0.03	
	Sculling	ACBZ	0.015 $\frac{cm}{sec^2}$	10		21	0.08		0.14
Cut-off Time Computation Effects	Uncoupled	$(E)V_{(alt)co}$	ft/sec						
	Vibration	$(E)V_{(tk)co}$	ft/sec						
	Effects	$(E)V_{(rge)co}$	0.10 ft/sec						0.10
RSS Error due to Vibration Effects				180	176	147	1.54	1.48	0.97
RSS Error due to Guidance & Initial Condition Errors exclusive of Vibration Effects				2,070	1,642	12,300	14.40	5.03	3.04

Table 7

Translunar Injection Trajectory Cutoff Errors
Due To Vibration Effects On Guidance

Effect Class	Error Effect	Equiv. Guid. Error Term	Avge. Equiv. Guid. Error	Position Error in Target Axes in ft.			Velocity Error in Target Axes in ft/sec		
				Alt.	Track	Range	Alt.	Track	Range
Linear Vibration Effects	Gyro	BDX	9.6 meru		40			0.38	
	Anisoelastic	BDY	9.6 meru	42		8	0.40		0.03
	(1 meru/g^2)	BDZ	9.6 meru		10			0.10	
	Gyro	BDX	0.05 meru		1			0.01	
	Cylindrical	BDY	0.05 meru	1		0	0.01		0
		BDZ	0.05 meru		0			0	
	Accelero-	ACBX	0.096 $\frac{cm}{sec^2}$	168		66	1.01		0.38
	meter Aniso-	ACBY	0.096 $\frac{cm}{sec^2}$		176			1.04	
	elastic ($10\mu g/g^2$)	ACBZ	0.096 $\frac{cm}{sec^2}$	66		163	0.40		0.98
Angular Vibration Effects	Gyro	BDX	0.10 meru		1			0.01	
	Coning & In-	BDY	0.05 meru	1		0	0.01		0
	Phase Motion	BDZ	0.10 meru		0			0	
Linear-Angular Vibration Effects	Accelero-	ACBX	0.015 $\frac{cm}{sec^2}$	26		11	0.15		0.06
	meter	ACBY	0.003 $\frac{cm}{sec^2}$		5			0.03	
	Sculling	ACBZ	0.015 $\frac{cm}{sec^2}$	11		26	0.06		0.15
Cutoff Time Computation Effects	Uncoupled	$(E)V_{(alt)co}$	---ft/sec						
	Vibration	$(E)V_{(tk)co}$	---ft/sec						
	Effects	$(E)V_{(rge)co}$	0.10 ft/sec						0.10
RSS Error due to Vibration Effects				188	180	179	1.17	1.10	1.07
RSS Error due to Guidance and Initial Condition Errors exclusive of Vibration Effects				2,550	1,075	7,870	5.53	3.23	2.94

Table 8

Lunar Orbit Insertion Trajectory Cutoff Errors
Due To Vibration Effects On Guidance
(CM-SM Configuration)

Effect Class	Error Effect	Equiv. Guid. Error Term	Avge. Equiv. Guid. Error	Position Error in Target Axes in. ft			Velocity Error in Target Axes in ft/sec		
				Alt.	Track	Range	Alt.	Track	Range
Linear Vibration Effects	Gyro	BDX	9.6 meru		6			0.11	
	Anisoelastic	BDY	9.6 meru	3		2	0.11		0.03
	(1 meru/g^2)	BDZ	9.6 meru		2			0.03	
	Gyro	BDX	0.05 meru		0			0	
	Cylindrical	BDY	0.05 meru	0		0	0		0
		BDZ	0.05 meru		0			0	
	Accelero-	ACBX	0.096 $\frac{cm}{sec^2}$	21		3	0.37		0.05
	meter Aniso-	ACBY	0.096 $\frac{cm}{sec^2}$		21			0.37	
	elastic (10$\mu g/g^2$)	ACBZ	0.096 $\frac{cm}{sec^2}$	3		21	0.05		0.37
Angular Vibration Effects	Gyro	BDX	0.10 meru		0			0	
	Coning & In-	BDY	0.05 meru	0		0	0		0
	Phase Motion	BDZ	0.10 meru		0			0	
Linear-Angular Vibration Effects	Accelero-	ACBX	0.015 $\frac{cm}{sec^2}$	3		1	0.06		0.01
	meter	ACBY	0.003 $\frac{cm}{sec^2}$		1			0.01	
	Sculling	ACBZ	0.015 $\frac{cm}{sec^2}$	1		3	0.01		0.06
Cutoff Time Computation Effects	Uncoupled	$(E)V_{(alt)co}$	ft/sec				0.03		0
	Vibration	$(E)V_{(tk)co}$	--ft/sec					0	
	Effects	$(E)V_{(rge)co}$	0.10 ft/sec				0		0.10
RSS Error due to Vibration Effects				22	22	22	0.40	0.39	0.45
RSS Error due to Guidance & Initial Condition Errors exclusive of Vibration Effects				370	543	2,554	2.21	1.48	0.95

Table 9

Transearth Injection Trajectory Cutoff Errors
Due To Vibration Effects On Guidance
(CM-SM Configuration)

Effect Class	Error Effect	Equiv. Guid. Error Term	Avge. Equiv. Guid. Error	Position Error in Target Axes in ft.		
				Alt.	Track	Range
Linear Vibration Effects	Gyro	BDX	58 meru		842	
	Anisoelastic	BDY	58 meru	898		178
	(1 meru/g^2)	BDZ	58 meru		346	
	Gyro	BDX	0.1 meru		3	
	Cylindrical	BDY	0.1 meru	3		1
		BDZ	0.1 meru		1	
	Accelero-	ACBX	0.57 $\frac{cm}{sec^2}$	1,870		375
	meter Aniso-	ACBY	0.57 $\frac{cm}{sec^2}$		1,825	
	elastic (10μg/g^2)	ACBZ	0.57 $\frac{cm}{sec^2}$	375		1,775
Angular Vibration Effects	Gyro	BDX	0.10 meru		1	
	Coning & In-	BDY	0.05 meru	1		0
	Phase Motion	BDZ	0.10 meru		1	
Linear-Angular Vibration Effects	Accelero-	ACBX	0.065 $\frac{cm}{sec^2}$	215		42
	meter	ACBY	0.015 $\frac{cm}{sec^2}$		45	
	Sculling	ACBZ	0.065 $\frac{cm}{sec^2}$	46		205
Cutoff Time Computation Effects	Uncoupled	$(E)V_{(alt)co}$	---ft/sec			
	Vibration	$(E)V_{(tk)co}$	---ft/sec			
	Effects	$(E)V_{(rge)co}$	---ft/sec			
RSS Error due to Vibration Effects				2,120	2,040	1,840
RSS Error due to Guidance & Initial Condition Errors exclusive of Vibration Effects				2,150	1.840	2,000

Table 10

LEM Lunar Descent Trajectory Cutoff Errors
Due To Vibration Effects On Guidance

Effect Class	Error Effect	Equiv. Guid. Error Term	Avge. Equiv. Guid. Error	Position Error in Target Axes in ft.			Velocity Error in Target Axes in ft/sec		
				Alt.	Track	Range	Alt.	Track	Range
Linear Vibration Effects	Gyro Anisoelastic (1 meru/g^2)	BDX	58 meru		468			4.49	
		BDY	58 meru	449		150	4.68		0.84
		BDZ	58 meru		84			0.19	
	Gyro Cylindrical	BDX	0.1 meru		1			0.01	
		BDY	0.1 meru	1		1	0.01		0
		BDZ	0.1 meru		0			0	
	Accelero- meter Aniso- elastic ($10\mu g/g^2$)	ACBX	0.57 $\frac{cm}{sec^2}$	1,095		159	6.45		1.03
		ACBY	0.57 $\frac{cm}{sec^2}$		1,085			6.17	
		ACBZ	0.57 $\frac{cm}{sec^2}$	159		1,066	1.03		6.17
Angular Vibration Effects	Gyro Coning & In- Phase Motion	BDX	0.10 meru		1			0.01	
		BDY	0.05 meru	1		0	0.01		0
		BDZ	0.10 meru		0			0	
Linear-Angular Vibration Effects	Accelero- meter Sculling	ACBX	0.065 $\frac{cm}{sec^2}$	127		20	0.75		0.10
		ACBY	0.015 $\frac{cm}{sec^2}$		30			0.15	
		ACBZ	0.065 $\frac{cm}{sec^2}$	20		124	0.10		0.54
Cutoff Time Computation Effects	Uncoupled Vibration Effects	$(E)V_{(alt)co}$	---ft/sec				0		0
		$(E)V_{(tk)co}$	---ft/sec					0	
		$(E)V_{(rge)co}$	0.08 ft/sec				0		0.08
RSS Error due to Vibration Effects				1,200	1,185	1,095	8.10	7.65	6.35
RSS Error due to Guidance & Initial Condition Errors exclusive of Vibration Effects				1,635	2,110	2,060	4.35	4.25	2.55

Table 11

LEM Lunar Ascent Trajectory Cutoff Errors
Due To Vibration Effects On Guidance

APPENDIX A

A.1 Linear Vibration Effects

A.1a IMU Gimbal Anisoelastic Effect

Gimbal anisoelasticity relative to a particular gimbal axis will, in the presence of linear vibration, give rise to a rectified disturbance torque about this axis. The resulting average Stable Member misalignment is a function of the gimbal servo torque constant and of the gimbal angle configuration. The average disturbance torque iteself is a function of the compliance difference (difference between the stiffnesses measured relative to the principal bending axes) and is proportional to the vibratory acceleration squared.

A.1b Gyro Anisoelastic Error

This gyro error is identical with the acceleration-squared sensitive drift rate error. It is caused by unequal stiffnesses of the gyro wheel assembly relative to the float along the principal stiffness axes. These axes are not necessarily colinear with the nominal gyro input and spin axes, although experimental tests show that they are not too far separated from these axes. Specifications for this error state that it may not exceed 1 meru/g^2 for accelerations along any direction. Experimental runs show that the average anisoelastic torque, and hence average g^2 sensitive drift, is close to maximum when the acceleration vector is at 45° relative to the gyro IA and SA axes. This average drift rate can be considered as equivalent to a gyro bias drift for a constant vibration input. Expressions for the three acceleration-squared drift rate terms follow:

$$A^2D_{(IA)(IA)} = \frac{m^2}{2H} (K_1 - K_2) \sin 2\mu$$

$$A^2D_{(SA)(SA)} = \frac{-m^2}{2H} (K_1 - K_2) \sin 2\mu$$

$$A^2D_{(IA)(SA)} = \frac{m^2}{2H} (K_1 - K_2) \cos 2\mu$$

where

m is float assembly mass

H is wheel angular momentum

$(K_1 - K_2)$ is compliance difference in inches/lb

μ is angle between principal stiffness axes and nominal gyro IA axis

Corresponding to the above stiffnesses are the gyro wheel-float natural frequencies, which are at about 1600 cps. Theoretical equations show that as vibration frequency approaches these natural frequencies the aniso-elastic torque increases to several hundred times the zero-frequency value. However, this should not be a problem, since vibrational energy should be very low at these high frequencies

A.1c Gyro Cylindrical Torque

This effect occurs when a gyro is subjected to a two-axis vibration normal to its output axis. If the two accelerations are equal and 90 degrees out-of-phase, the output axis is made to describe a cylinder in space. The net effect is a rotating acceleration vector. At or near zero frequency the net average torque, due to the deflection of the gyro wheel relative to the float lagging the acceleration vector, is zero. However, as the first resonant frequency is approached (see previous section) a net cylindrical torque develops, since the deflection lags the acceleration vector by about 90°. A peak cylindrical torque is reached at the first natural frequency and again at the second natural frequency. However, since the vibrational energy is low at these relatively high frequencies, the average cylindrical torque, and the corresponding average gyro drift, is relatively low

A.1d Accelerometer Anisoelastic Error

This accelerometer error is identical with the acceleration-squared sensitive indication error. It is proportional to the difference of the two PIPA float stiffnesses along principal axes normal to the output axis. Vibratory acceleration normal to the output axis will produce a rectified torque about the output axis that is a function of the compliance difference. The average indication error due to this effect can be considered as equivalent to an accelerometer bias error, as long as the vibration environment remains constant.

A.2 Angular Vibration Effects

A.2a Gyro Coning Due to SM Quadrature Motion

When a gyro input axis is made to describe a cone in space, there will be net angular velocity about the ideal input axis that will be sensed by the gyro. Since the gyro ideally is not rotating about its input axis, this net angular rate must be considered an error or drift rate that is not caused by any property of the gyro itself.

This net drift rate is given by

$$W = \frac{\phi_{am}\,\phi_{bm}\,w}{2}$$

where ϕ_{am} and ϕ_{bm} are the angular vibration amplitudes about orthogonal directions normal to the input axis, and where w is the vibration frequency.

As vibration frequency is increased, there is an attenuation of the gyro float's response to the vibration input and also a phase shift. Because of these effects the drift rate due to coning motion rises to a peak at a frequency equal to the reciprocal of the gyro time constant (about 210 cps for the Apollo IRIG) and then falls off with increasing vibration frequency.

A.2b Gyro Anisoinertia and Kinematic Rectification Due to SM In-Phase Motion

For in-phase angular vibrations about the gyro input and spin axes a rectified torque will develop about the output axis proportional to the differences in float moment of inertia about the spin and input axes. This rectified torque will produce an average drift rate. The drift rate caused by anisoinertia is insignificant for vibration frequencies under 200 cps, and becomes the dominant drift rate factor for frequencies over 400 cps.

In addition to the anisoinertia effect there is a kinematic rectification effect due to in-phase vibrations about the gyro input and spin axes that also results in an average drift rate. This is also insignificant at frequencies less than 100 cps. For a detailed study of this and other vibration effects the reader is referred to MIT/IL Report E-1399*.

*Weinstock, Robert, The Effects of Vibration on Gyroscope Instruments, M.I.T. Instrumentation Laboratory Report E-1399, August 1963 (U).

The peak response of the Stable Member to oscillatory friction torques is at about 16 cps. At this frequency the coning effect, which can only occur with quadrature motion, is by far the dominant drift rate contributor.

A.3 Combined Linear-Angular Vibration Effects

A.3a Accelerometer Sculling

Accelerometer sculling is a combination of linear vibration along one direction normal to the accelerometer input axis combined with angular vibration about a third axis normal to the first two. When the linear and angular vibrations are in-phase, the accelerometer output will include an average indication error due to rectified cross-coupling. For a constant linear and angular vibration environment, this average indication error can be considered equivalent to an accelerometer bias error.

A.4 Cutoff Time Computation Effects

A.4a Uncoupled Vibration Effects

Ideally the accelerometers should measure the acceleration of the spacecraft center of gravity. However, since the Stable Member is mounted on gimbals in the IMU attached to the navigation base that is in turn mounted on the spacecraft frame, the accelerometers will actually sense linear vibration due both to linear and to angular vibrations that are not sensed by the spacecraft center of gravity. An error in cutoff time computation can be caused due to the presence of these decoupled vibration effects.

A.4b Cross-Coupling Due to SM Angular Vibration

If the Stable Member is undergoing angular vibrations the accelerometers, which are oriented approximately normal to the thrust acceleration vector, will include as part of their output an oscillatory indication error that is equal to the product of the instantaneous SM angular vibration amplitude and the thrust acceleration. This instantaneous cross-coupling error can cause an error in cutoff time computation. This error should, however, be insignificant unless angular vibration amplitudes are much greater than anticipated.

DISTRIBUTION LIST

Internal

R. Alonso
J. Arnow (Lincoln)
R. Battin
W. Bean
E. Berk
P. Bowditch
A. Boyce
R. Boyd
G. Bukow
G. Cherry
E. Copps
R. Crisp
W. Crocker
J. Dahlen
E. Duggan
K. Dunipace (MIT/AMR)
J. B. Feldman
Julius Feldman
P. Felleman
S. Felix (MIT/S&ID)
J. Flanders
J. Fleming
F. Grant
Eldon Hall
E. Hickey
D. Hoag
A. Hopkins
F. Houston
L. B. Johnson
M. Johnston
A. Koso
M. Kramer
A. Laats
A. La Pointe
J. Larsen
L. Larson
J. Lawrence (MIT/GAEC)
T. J. Lawton
T. M. Lawton (MIT/MSC)
D. Lickly
G. Mayo
J. McNeil
R. McKern
James Miller
John Miller
J. Nevins
J. Nugent
E. Olsson
C. Parker
W. Patterson
J. Rhode
K. Samuelian
G. Schmidt
R. Scholten
E. Schwarm
J. Sciegienny
N. Sears
J. Shillingford
W. Shotwell (MIT/ACSP)
T. Shuck
J. Sitomer
J. Stone
J. Suomala
W. Tanner
N. Thacher
R. Therrien
W. Toth
M. Trageser
R. Weatherbee
R. White
L. Wilk
R. Woodbury
W. Wrigley
Apollo Library (2)
MIT/IL Library (6)

External

(ref. PP1-64; April 8, 1964)

P. Ebersole (NASA/MSC)		(2)
W. Rhine (NASA/RASPO)		(1)
L. Holdridge (NAA S&ID/MIT)		(1)
T. Heueremann (GAEC/MIT)		(1)
AC Spark Plug		(10)
Kollsman		(10)
Raytheon		(10)
Major W. Delaney (AFSC/MIT)		(1)
NAA RASPO:	National Aeronautics and Space Administration Resident Apollo Spacecraft Program Office North American Aviation, Inc. Space and Information Systems Division 12214 Lakewood Boulevard Downey, California	(1)
FO:	National Aeronautics and Space Administration, MSC Florida Operations, Box MS Cocoa Beach, Florida 32931 Attn: Mr. B. P. Brown	(3)
HDQ:	NASA Headquarters 600 Independence Ave., SW Washington 25, D. C. 20546 Attn: MAP-2	(6)
AMES:	National Aeronautics and Space Administration Ames Research Center Moffett Field, California Attn: Library	(2)
LEWIS:	National Aeronautics and Space Administration Lewis Research Center Cleveland, Ohio Attn: Library	(2)
FRC:	National Aeronautics and Space Administration Flight Reserach Center Edwards AFB, California Attn: Research Library	(1)
LRC:	National Aeronautics and Space Administration Langley Research Center Langley AFB, Virginia Attn: Mr. A. T. Mattson	(2)

GSFC:	National Aeronautics and Space Administration Goddard Space Flight Center Greenbelt, Maryland Attn: Manned Flight Support Office Code 512	(2)
MSFC:	National Aeronautics and Space Administration George C. Marshall Space Flight Center Huntsville, Alabama Attn: R-SA	(2)
ERC:	National Aeronautics and Space Administration Electronics Research Center 575 Technology Square Cambridge, Massachusetts Attn: R. Hayes/A. Colella	(1)
GAEC:	Grumman Aircraft Engineering Corporation Bethpage, Long Island, New York Attn: Mr. A. Whitaker	(1)
NAA:	North American Aviation, Inc. Space and Information Systems Division 12214 Lakewood Boulevard Downey, California Attn: Mr. R. Berry	(1)
GAEC RASPO:	National Aeronautics and Space Administration Resident Apollo Spacecraft Program Officer Grumman Aircraft Engineering Corporation Bethpage, L.I., New York	(1)
ACSP RASPO:	National Aeronautics and Space Administration Resident Apollo Spacecraft Program Officer Dept. 32-31 AC Spark Plug Division of General Motors Milwaukee 1, Wisconsin Attn: Mr. W. Swingle	(1)
WSMR:	National Aeronautics and Space Administration Post Office Drawer MM Las Cruces, New Mexico Attn: BW 44	(1)
MSC:	National Aeronautics and Space Administration Manned Spacecraft Center Apollo Document Control Group Houston 1, Texas 77058	(45)
	Mr. H. Peterson Bureau of Naval Weapons c/o Raytheon Company Foundry Avenue Waltham, Massachusetts	(1)

Queens Material Quality Section (1)
c/o Kollsman Instrument Corp.
Building A 80-08 45th Avenue
Elmhurst, New York 11373
Attn: Mr. S. Schwartz

Mr. H. Anschuetz (1)
USAF Contract Management District
AC Spark Plug Division of General Motors
Milwaukee, Wisconsin 53201